ACS APPLIED MATERIALS & INTERFACES

Research Article

www.acsami.org

Strain-Tunable One Dimensional Photonic Crystals Based on Zirconium Dioxide/Slide-Ring Elastomer Nanocomposites for Mechanochromic Sensing

Irene R. Howell,[†] Cheng Li,[†] Nicholas S. Colella,[†] Kohzo Ito,[‡] and James J. Watkins*[,†]

[†]Center for Hierarchical Manufacturing, Department of Polymer Science and Engineering, University of Massachusetts Amherst, 120 Governors Drive, Amherst, Massachusetts 01003, United States

[‡]Department of Advanced Materials Science, GSFS, University of Tokyo 5-1-5 Kashiwano-ha, Kashiwa, Chiba 277-8561, Japan

Supporting Information

ABSTRACT: We demonstrate the fabrication and performance of tunable, elastic organic/inorganic composite one-dimensional photonic crystals (1DPCs) in the visible spectrum. By controlling the composition of high refractive index metal oxide nanoparticle/polymer composites, a refractive index difference of 0.18 between the filled and unfilled polymer layers can be achieved while maintaining desirable flexibility and elasticity. This index contrast is achieved with a loading of 70 wt % zirconium dioxide nanoparticles within a slide-ring elastomer matrix, which is composed of topologically cross-linked polyrotaxane polyols. The large refractive index contrast enables high reflectivity while simultaneously minimizing the number of layers necessary, compared to purely polymer systems. Because the films are both flexible and elastic, these nanocomposite 1DPCs can function as colorimetric strain sensors. We demonstrate the sensing behavior of these 1DPCs by applying over 40% strain, resulting in a visible color shift across the visible spectrum from red to blue. 1DPCs of just 6 periods maintain reflectance of 40% throughout the visible spectrum, with a tensile mechanochromic sensitivity ($\Delta\lambda/\Delta\varepsilon_{max}$) as high as −6.05 nm/%.

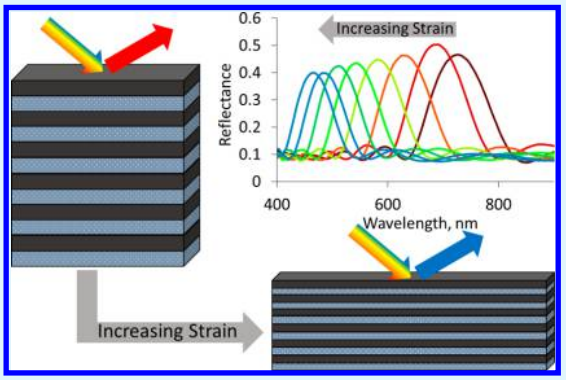

KEYWORDS: *one dimensional photonic crystal, Bragg mirror, colorimetric sensor, elastomer-nanoparticle composite, slide-ring elastomer, high refractive index composite*

INTRODUCTION

Since the landmark publications of John[1] and Yablonovitch,[2] one-dimensional photonic crystals (1DPCs) have been studied and applied in LEDs,[3] photovoltaics,[4] lasers,[5] and sensors.[6] 1DPCs consist of layers of alternating high and low refractive index materials and, based on their periodic structure, exhibit a photonic stop-band in which a range of wavelengths is forbidden from propagating through the medium.[7] Constructive interference due to the structure's periodicity gives rise to an intense reflection in the stop-band. Each period consists of a layer of high and a layer of low refractive index material, each with optical thickness $\lambda/4$. The contrast in refractive index and the number of periods contribute to the intensity of the reflected wavelengths. Therefore, adequate contrast in refractive indices and sufficient numbers of layers are required to provide high levels of reflection.

Thin films for 1DPCs have been fabricated from methods including chemical and physical vapor deposition as well as sputtering.[7] These methods generally require high temperatures and/or vacuum conditions and are thus suitable for producing thin films from inorganic materials including metals or semiconductors but are not be suitable for organic materials such as polymers, due to their temperature limitations. Although inorganic materials may provide a wide spectrum of refractive indices, due to their inherent rigidity, harsh processing conditions, as well as limitations for use in the visible region of the electromagnetic spectrum, we focus on polymer-based thin film composites.

Polymer-based Bragg mirrors are attractive due to their flexibility, processability, and transparency in the visible region. Because polymers have a relatively limited range of refractive indices, usually close to 1.5, purely polymer systems often require a large number of periods for sufficient reflection. One method for achieving these many layers is through polymer self-assembly. Edrington et al. describe the use of block copolymers to create photonic crystals,[8] whereby block copolymers of a specified composition will phase separate into a lamellar morphology, giving rise to a one-dimensional periodic structure. If the domain sizes are large enough, wavelengths of practical interest, i.e., UV, Vis, or IR, may be reflected. In order to achieve these large domain sizes, block copolymer and homopolymer blends have been used[9] as well as

Received: November 14, 2014
Accepted: January 26, 2015
Published: January 26, 2015

DOI: 10.1021/am5079946
ACS Appl. Mater. Interfaces 2015, 7, 3641−3646

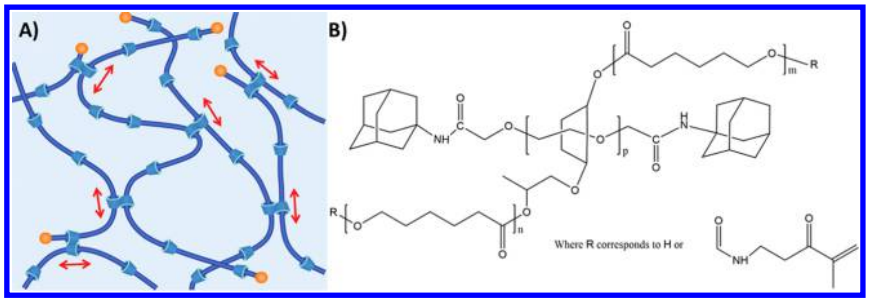

Figure 1. (A) Schematic structure of slide-ring elastomers. The polymer chains are connected topologically by figure-of-eight cross-links and are freely moveable. Adapted from ref 20. Copyright 2011 American Chemical Society. (B) The chemical structure of SeRM Super Polymer AU1000 is shown. Once interlocked with other chains, these form the slide-ring network.

bottle brush block copolymers.[10] Additionally, the incorporation of high refractive index nanoparticles into a polymer matrix provides another way to achieve sufficient reflection for photonic applications.[11,12] Miguez et al. describe a unique method for creating polymer-infiltrated nanoparticle layers, resulting in highly reflecting, flexible 1DPCs with 6 periods; however, strain tuning properties of these materials were not reported.[13] Kolle et al. demonstrates the concept of stretch-tunable 1DPCs using a purely polymer system.[14] In this work we utilize the advantage offered by nanoparticles in reducing the number of periods required for significant reflection as well as those of using an elastic polymer host to create flexible and stretchable nanocomposite tunable 1DPCs.

Recently, many polymer-based one and three-dimensional photonic crystals have been used to fabricate mechanochromic sensors: sensors that respond to an external mechanical stimulus with a variation in color. Typical values of sensitivity, defined as the shift in the wavelength of peak reflectance divided by the applied strain (nm/%), for these sensors ranges from 0.7 to 5.3 and are dependent on the type of force applied and the material systems.[15] Much of the focus is on photonic gels, as gels have exhibited higher sensitivities.[15,16] Gels, however, rely on solvent-induced swelling; in this work, we choose to use elastomer sensors which are suitable for diverse environments that would be unsuitable for solvent-dependent gel sensors.

Specifically, we demonstrate the use of highly filled elastomer nanocomposites for use in stretchable photonic applications. The structure of the slide-ring elastomers chosen for this work is shown in Figure 1 and consists of cyclodextrin molecules which have been functionalized for UV-cross-linking and threaded onto poly(ethylene glycol) chains. The moveable cyclodextrin cross-links allow for distribution of stress not possible in chemically and physically cross-linked materials. This effect is referred to as the "pulley effect".[17] These materials are good candidates because they exhibit low shrinkage, high flexibility, scratch resistance, stress-relaxation, as well as reduction of hysteresis losses.[18] The commercially available polymer resins used in this work consist of a blend of the polymers and reactive acrylates.[19] Additionally, because of their unique supramolecular structure, these elastomers have applications in scratch resistant coatings, dielectric elastomers, and vibration absorption materials.[18] Of particular note, due to the high flexibility of these polymers,[17] extensibility can be maintained despite significant loading of metal oxide nanoparticles.

RESULTS AND DISCUSSION

Well dispersed ZrO_2 nanocrystals were mixed with UV-curable slide-ring elastomer resins and a photoinitiator in a toluene solution. Solutions were spin-cast and the proper film thicknesses were achieved by controlling the spin coating rpm and the weight percent of polymer and nanopartilces in solution. In order to determine the suitability of the nanoparticles for optical applications, the transparency of the composites was considered. Transmittance measurements were taken for composites containing 70 wt % ZrO_2. Because of the layered nature of the final structure, transmittance measurements were taken of five layers of composite material that had been consecutively spin coated and UV-cured. The transmittance spectrum, shown in Figure 2A, indicated excellent transparency of the composites. The layered films retained transparency above 94% in the visible spectrum. This transparency, even at a high loading of particles, arose from the nanoparticles' small size and good dispersibility within the polymer host. The nanoparticles, with average diameters centered at 6 nm, were small enough to avoid scattering of incident light. The TEM image in Figure 2B shows results consistent with the supplier (diameter 6 nm). Additionally, no aggregation is observed which would lead to scattering. The TEM sample was prepared by floating a composite film directly onto a copper grid.

The refractive index of the materials was measured over the visible spectrum for various weight percentages of ZrO_2 in the elastomer matrix. By incorporating high refractive index nanoparticles, we show that the composite refractive index can be increased, resulting in good refractive index contrast for the 1DPCs. Figure 3A shows the refractive index as a function of weight and volume percent of ZrO_2. The refractive index increased linearly with increasing nanoparticle volume percent, as expected.[11] The refractive index at 70 wt % (30 vol %) was 1.68. This provided a refractive index difference of 0.18.

1DPCs were fabricated by spin coating and UV-curing layers of filled and unfilled elastomer resins, forming bilayers. These bilayers were lifted and stacked on each other by using a water-soluble sacrificial base layer. The SEM image in Figure 3B shows an example of a 5 bilayer 1DPC coated directly above a water-soluble sacrificial layer, all on top of a silicon wafer. Figure 3B shows an early 1DPC, fabricated by spin coating each layer directly on top of the previous without lifting and stacking individual bilayers (see the Experimental Section). The increased electron scattering caused by the nanoparticles in the filled layers gave rise to the brighter appearance of the high-index layers. 1DPCs with thicknesses designed to reflect in the

DOI: 10.1021/am5079946
ACS Appl. Mater. Interfaces 2015, 7, 3641−3646

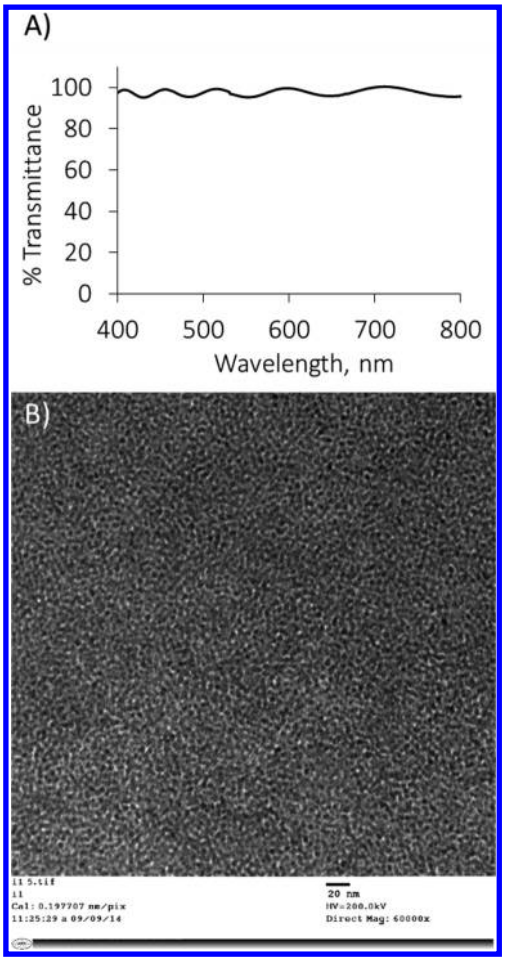

Figure 2. (A) Transmission spectra of 5 layers of 70 wt % ZrO_2 in a UV-cured slide ring elastomer. (B) TEM image of ZrO_2 nanoparticles dispersed within a slide ring elastomer matrix at 70 wt % nanoparticles.

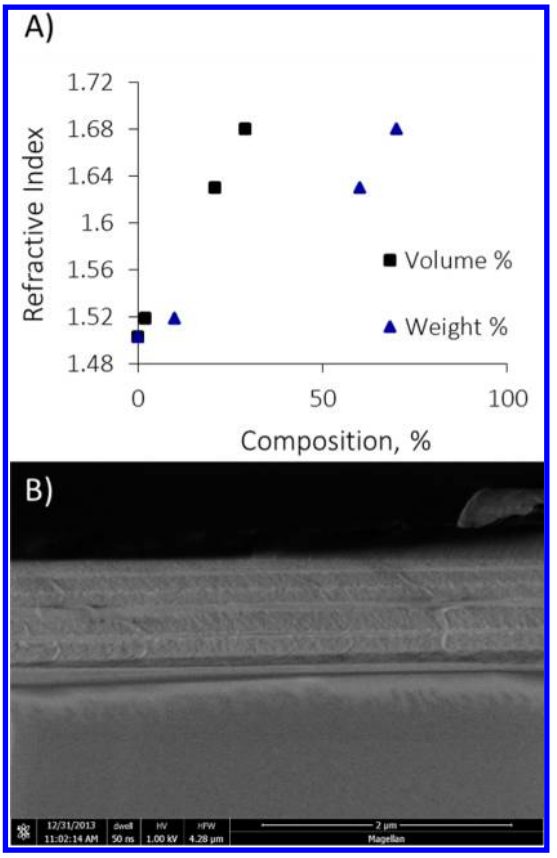

Figure 3. (A) Refractive index of various nanocomposite compositions. (B) SEM image of a 5 bilayer 1DPC consisting of alternating filled (70 wt % ZrO_2) and unfilled slide-ring elastomers. The bottom-most layer is a water-soluble sacrificial layer of poly(vinyl alcohol) on silicon.

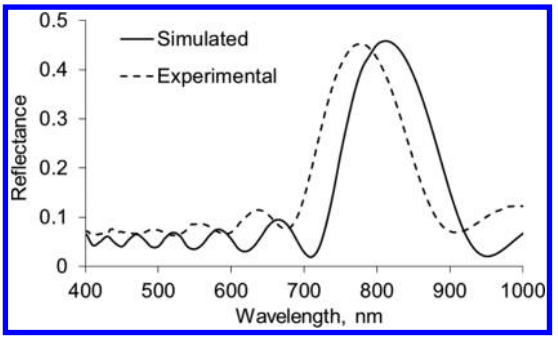

Figure 4. Simulated and experimental reflectance spectrum for 70 wt % ZrO_2 composite 1DPCs containing 6 periods.

red region of the visible spectrum were fabricated according to the following criteria:

$$\lambda_0/4 = n_H t_H = n_L t_L \quad (1)$$

where the optical thicknesses of the high index layer and low index layer are equal to each other as well as to one-fourth of the wavelength to be reflected. Appropriate rotational speeds and concentrations of solutions were used in order to achieve the desired thicknesses via spin coating (see the Experimental Section).

Film thickness was determined by variable angle spectroscopic ellipsometry and was used to measure simultaneously the individual thicknesses of the water-soluble polymer layer, the ZrO_2-filled elastomer layer, and the unfilled elastomer layer. The change in phase and amplitude of the incident polarized light were measured by the ellipsometer and then fit to a Cauchy model to determine thickness. The thicknesses measured from this method were 110 and 121 nm for the filled and unfilled layers, respectively, with an expected variation in film thickness on the order of 5 nm (see the Supporting Information, Figure S1). Finite element analysis using COMSOL Multiphysics predicted a reflectance peak of 45.8% centered at 810 nm from a 1DPC composed of six bilayers of ZrO_2-filled and unfilled elastomer, which is in good agreement with the experimental results that showed a reflectance peak of 45.2% at 775 nm. Figure 4 shows the results of the simulation alongside the experimental reflectance measurements. The highest values of reflectance will be observed when the layer thicknesses perfectly adhere to the stipulations of eq 1; therefore, the slight discrepancy between experimental and simulated results may be attributed to unavoidable minor variations in layer thicknesses. Additionally, the reflectance intensity and bandwidth of the simulated and experimental results match very closely. Since the solutions to Maxwell's equations for electromagnetism in dielectric materials have no fundamental length scale,[21] the reflectance intensity and bandwidth match despite a difference in peak location.

In order to measure the response of the 1DPC to strain, a simple stretching device was constructed to fit beneath the

DOI: 10.1021/am5079946
ACS Appl. Mater. Interfaces 2015, 7, 3641−3646

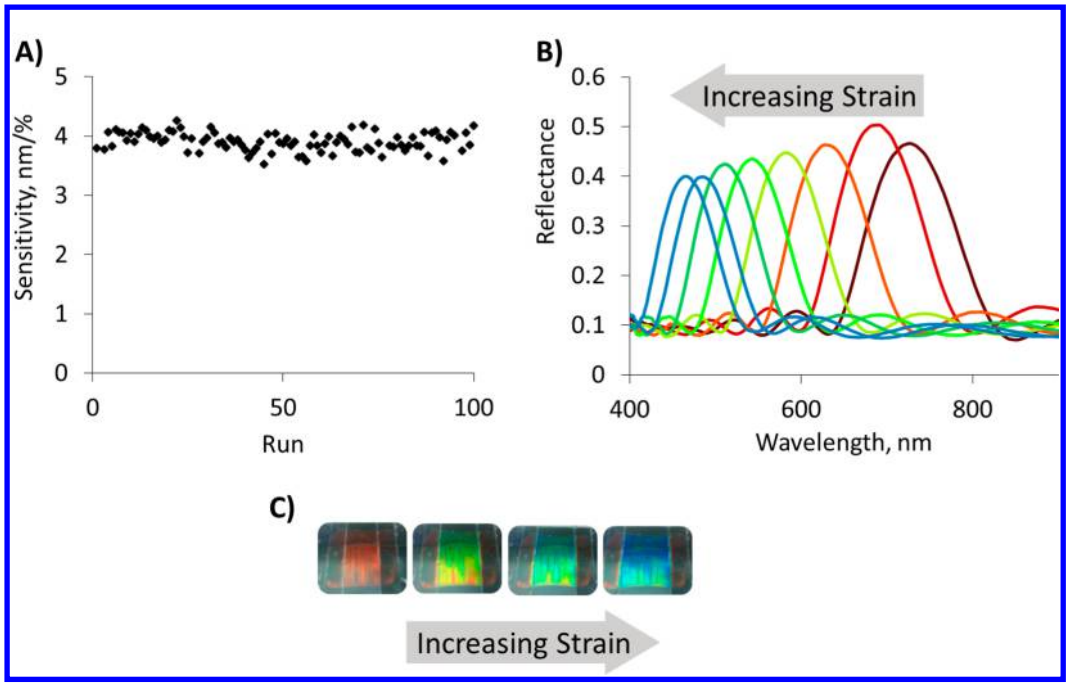

Figure 5. (A) Mechanochromic sensitivity of 6 period 1DPC over 100 runs after 4 months at a set strain of less than 10%. (B) Reflectance spectra of a 6 period 1DPC under increasing strain. The furthest right peak corresponds to zero strain; the furthest left peak corresponds to strain of 0.42 (42%). (C) Digital photographs of 6 layer 1DPC under increasing strain from 0% (red) to approximately 40% (blue). Though measurements were taken at 90°, photographs were taken in a broadly lit room and the angle was chosen in order to best convey the color observed under 90° incident light.

reflectometer in order to take measurements as strain was applied to the film. All measurements were taken at 90° relative to the sample surface with strain varying from 0 to 42%. Figure 5B shows the shift in wavelength of peak reflectance as strain is applied. The reflectance peak shifts to shorter wavelengths as strain on the film is increased. The applied tensile strain corresponds to compression in the direction normal to the plane of the applied strain, causing the thickness to decrease, thereby blue-shifting the reflectance peak in accordance with eq 1. The color of the 1DPCs visibly changes from red to blue as the film is stretched, as shown in Figure 5C. Though some discoloration is observed, particularly near the edges of the 10 by 17 mm film due to defects resulting from handling and fabrication, the color in the center area (of at least 50 mm^2) of the sensor remains consistent.

Mechanochromic sensitivity, defined as peak shift per percent strain, provides a useful metric for characterizing various sensor material systems.[22] While the highest reported sensitivity is 12 nm/% for a lamellar block copolymer system in compression, the mechanochromic sensitivity of block copolymer gels in uniaxial tension ranged in magnitude from 0.7 to 5.25 nm/%.[23] As shown in Table 1, the 1DPCs reported here demonstrate a maximum mechanochromic sensitivity as large at −6.05 nm/% for uniaxial tension. However, though the magnitude of the initial sensitivity is 6.05 nm/%, the value decreased after the sensor was left strained over several months (see Figure 5A). The sensitivity decreased to 3.9 ± 0.16 nm/% and remained consistent over more than 100 cycles. Strains of 40% were applied repeatedly without failure, indicating excellent reusability. Assuming the alternating layers are composed of material of similar thickness and modulus, the theoretical sensitivity for the 1DPC was calculated as −7.33 using the following equation[23]

$$\lambda(\varepsilon_z) = (2n_H t_H + 2n_L t_L)(1 + \varepsilon_z) \quad (2)$$

where ε_z corresponds to the applied strain. For rubbery materials, Poisson's ratio approaches 0.5 as stiffness decreases. The great sensitivity of these 1DPCs may be attributed to the unique softness of the slide-ring materials[24] used as the matrix.

Table 1. 1DPC Mechanochromic Sensitivity

run	$\Delta\varepsilon_{max}$, %	$\Delta\lambda$, nm	sensitivity, $\Delta\lambda/\Delta\varepsilon_{max}$
1	43.3	−261.12	−6.05
2	43.2	−238.31	−5.57
3	42.5	−234.58	−5.52
4	42.5	−223.75	−5.26
100 runs averaged	39.3 ± 1.7	−153.3 ± 3.4	−3.9 ± 0.16

CONCLUSION

We have demonstrated the use of polymer/nanoparticle composite materials for unique optical sensor materials. The refractive index of polymer materials was modified by incorporating high refractive index nanoparticles, thus reducing the number of layers required to generate sufficient reflection. The use of UV-curable slide ring elastomers as the matrix allowed for high loadings of 6 nm ZrO_2 nanoparticles to be incorporated into the matrix while maintaining transparency, flexibility, and extensibility. These composite materials were used to construct strain-tunable 1DPCs, comprised of just 6 periods, which exhibited reflectance above 40% and maximum mechanochromic sensitivity of over 6 nm/% strain.

EXPERIMENTAL SECTION

Materials. Slide ring elastomer resins were donated by Advanced SoftMaterials Inc.; the UV-curable SA2400C resin was used in these experiments. Photoinitiator Irgacure 819 was purchased from BASF.

DOI: 10.1021/am5079946
ACS Appl. Mater. Interfaces 2015, 7, 3641−3646

Zirconia nanocrystals dispersed in toluene were purchased from Pixelligent. Poly(vinyl alcohol) (PVOH, Mowiol 4-88) was purchased from Sigma-Aldrich. The 89 000 MW polystyrene-*block*-poly(ethylene-*ran*-butylene)-*block*-polystyrene (SEBS) was purchased from Sigma-Aldrich.

1DPC Fabrication. 1DPCs were fabricated by sequential stacking of multiple bilayers. For each bilayer, a water-soluble sacrificial layer was coated onto a silicon wafer using 5 wt % PVOH in water onto a silicon wafer at 3000 rpm for 1 min. The PVOH layer was then baked at 110 °C for 1 min to evaporate residual water. For the high refractive index layer, ZrO_2 was added to a 2.5 wt % SA2400C toluene solution to achieve a 70% ZrO_2 solution (with respect to total weight of solids). The 1 wt % (with respect to the weight of SA2400C) of Irgacure 819 was added from a 5 wt % photoinitiator solution. This solution was mixed and exposure to light was minimized. For the low refractive index layer, a 5 wt % solution of SA2400C and 1 wt % Irgacure 819 in toluene was used. The nanoparticle-filled layer was spin coated onto the PVOH layer at 5000 rpm for 20 s and then UV-cured using OAI UV light source with emission peak at 365 nm and intensity of 17 mJ/cm^2. Following the cure, the unfilled polymer solution was spin coated at 3000 rpm for 20 s and then cured. This was repeated on six substrates simultaneously, in order to minimize any time variation of the polymer−nanoparticle solutions and to make sure the bilayer thicknesses were consistent. The substrates were placed top down onto an approximately 150 μm thick transparent SEBS thermoplastic elastomer substrate. Elastomer substrates were prepared by blade coating from 20 wt % solutions in toluene. Water was pipetted around the perimeter of the silicon substrate and covered to keep undisturbed for 1 h. After an hour, the PVOH layer had dissolved, leaving the bilayer film in contact with the elastic substrate. This process was repeated for each bilayer to build a 6 bilayer 1DPC.

1DPC Characterization. An aluminum frame was designed to hold and stretch the 1DPC while taking reflectance measurements. Two translation stages (Altos Photonics) were attached to an aluminum plate opposite each other, with the 1DPC secured between them. Using a Filmetrics F20, baseline measurements were taken using a silicon wafer and then reflectance measurements of the 1DPC were taken while the film was unstrained and at various strain percentages. Changes in length across the 10 mm × 17 mm 1DPC were measured using digital calipers and used to calculate strain.

■ ASSOCIATED CONTENT

Ⓢ Supporting Information

Clarification of film thickness measurements. This material is available free of charge via the Internet at http://pubs.acs.org.

■ AUTHOR INFORMATION

Corresponding Author

*E-mail: watkins@polysci.umass.edu.

Author Contributions

The manuscript was written through contributions of all authors.

Notes

The authors declare no competing financial interest.

■ ACKNOWLEDGMENTS

Funding was provided by the NSF Center for Hierarchical Manufacturing (Grant CMMI-1025020) and the G8 Research Councils Initiative on Multilateral Research through the NSF (Grant CMMI-1258336) and is gratefully acknowledged. We also thank Feyza Dündar for the TEM images.

■ REFERENCES

(1) John, S. Strong Localization of Photons in Certain Disordered Dielectric Superlattices. *Phys. Rev. Lett.* **1987**, *58*, 2486−2489.
(2) Yablonovitch, E. Inhibited Spontaneous Emission in Solid-State Physics and Electronics. *Phys. Rev. Lett.* **1987**, *58*, 2059−2062.
(3) Hunt, N. E. J.; Schubert, E. F.; Logan, R. A.; Zydzik, G. J. Enhanced Spectral Power Density and Reduced Linewidth at 1.3 um in an InGaAsP Quantum Well Resonant-Cavity Light-Emitting Diode. *Appl. Phys. Lett.* **1992**, *61*, 2287−2289.
(4) Colodrero, S.; Mihi, A.; Haggman, L.; Ocana, M.; Hagfeldt, A.; Miguez, H. Porous One-Dimensional Photonic Crystals Improve the Power-Conversion Efficiency of Dye-Sensitized Solar Cells. *Adv. Mater.* **2008**, *21*, 764−770.
(5) Calvez, S.; Hastie, J.; Guina, M.; Okhotnikov, O.; Dawson, M. Semiconductor Disk Lasers for the Generation of Visible and Ultraviolet Radiation. *Laser Photon. Rev.* **2009**, *3*, 407−434.
(6) Chiappelli, M.; Hayward, R. Photonic Multilayer Sensors from Photonic-Crosslinkable Polymer Films. *Adv. Mater.* **2012**, *24*, 6100−6104.
(7) Macleod, H. A. *Thin Film Optical Filters*, 3rd ed; Institute of Physics Publishing: London, 2001.
(8) Edrington, A.; Urbas, A.; DeRege, P.; Chen, C.; Swager, T.; Hadjichristidis, N.; Xenidou, M.; Fetters, L.; Joannopoulos, J.; Fink, Y.; Thomas, E. Polymer-based Photonic Crystals. *Adv. Mater.* **2001**, *13*, 421−425.
(9) Urbas, A.; Sharp, R.; Fink, Y.; Thomas, E.; Xenidou, M.; Fetters, L. Tunable Block Copolymer/Homopolymer Photonic Crystals. *Adv. Mater.* **2000**, *12*, 812−814.
(10) Sveinbjornsson, B.; Weitekamp, R.; Miyake, G.; Xia, Y.; Atwater, H.; Grubbs, R. Rapid Self-Assembly of Brush Block Copolymers to Photonic Crystals. *Proc. Natl. Acad. Sci. U.S.A.* **2012**, *109*, 14332−14336.
(11) Caseri, W. Nanocomposites of Polymers and Metals or Semiconductors: Historical Background and Optical Properties. *Macromol. Rapid Commun.* **2000**, *21*, 705−722.
(12) Beaulieu, M.; Hendricks, N.; Watkins, J. Large-Area Printing of Optical Gratings and 3D Photonic Crystals Using Solution-Processable Nanoparticle/Polymer Composites. *ACS Photon.* **2014**, *1*, 799−805.
(13) Calvo, M.; Miguez, H. Flexible, Adhesive, andBiocompatible Bragg Mirrors Based on Polydimethylsiloxane Infiltrated Nanoparticle Multilayers. *Chem. Mater.* **2010**, *22*, 3909−3915.
(14) Kolle, M.; Zheng, B.; Gibbons, N.; Baumberg, J.; Steiner, U. Stretch-tuneable Dielectric Mirrors and Optical Microcavities. *Opt. Express.* **2010**, *18*, 4356−4364.
(15) Chan, P.; Walish, J.; Urbas, A.; Thomas, E. Mechanochromic Photonic Gels. *Adv. Mater.* **2013**, *29*, 3934−3947.
(16) Yue, Y.; Kurokawa, T.; Haque, M.; Nakajima, T.; Nonoyama, T.; Li, X.; Kajiwara, I.; Gong, J. Mechano-actuated ultragast full-colour switching in layered photonic hydrogels. *Nat. Commun.* **2014**, *5*, 4659.
(17) Ito, K. Slide-Ring Materials using Topological Supramolecular Architecture. *Curr. Opin. Solid State Mater. Sci.* **2010**, *14*, 28−34.
(18) Noda, Y.; Hayashi, Y.; Ito, K. From topological gels to slide-ring materials. *J. Appl. Polym. Sci.* **2014**, *131*, 40509.
(19) Araki, J.; Ito, K. Recent Advances in the Preparation of Cyclodextrin-Based Polyrotaxanes and Their Applications to Soft Materials. *Soft Mater.* **2007**, *3*, 1456−1473.
(20) Bitoh, Y.; Akuzawa, N.; Urayama, K.; Takigawa, T.; Kidowaki, M.; Ito, K. Peculiar Nonlinear Elasticity of Polyrotaxane Gels with Moveable Cross-links Revealed by Multiaxial Stretching. *Macromolecules* **2011**, *44*, 8661−8667.
(21) Joannopoulos, J.; Johnson, S. G.; Winn, J. N.; Meade, R. D. *Photonic Crystals: Molding the Flow of Light*, 2nd ed.; Princeton University Press: Princeton, NJ, 2008.
(22) Lee, J.-H.; Koh, C. Y.; Singer, J. P.; Jeon, S.-J.; Maldovan, M.; Stein, O.; Thomas, E. 25th Anniversary Article: Ordered Polymer Structures for the Engineering of Photons and Phonons. *Adv. Mater.* **2014**, *26*, 532−569.
(23) Chan, E. P.; Walish, J. J.; Thomas, E. L.; Stafford, C. M. Block Copolymer Photonic Gel for Mechanochromic Sensing. *Adv. Mater.* **2011**, *23*, 4702−4706.

DOI: 10.1021/am5079946
ACS Appl. Mater. Interfaces 2015, 7, 3641−3646

(24) Ito, K. Novel Entropic Elasticity of Polymeric Materials: Why is Slide-Ring Gel So Soft? *Polym. J. (Tokyo, Jpn.)* **2012**, *44*, 38−41.

DOI: 10.1021/am5079946
ACS Appl. Mater. Interfaces 2015, 7, 3641−3646